Gold Passivated Mechanically Flexible Interconnects (MFIs) with High Elastic Deformation

Chaoqi Zhang, Hyung Suk Yang, and Muhannad S. Bakir
School of Electrical and Computer Engineering
Georgia Institute of Technology, Atlanta, Georgia, 30332
Email: chqzhang@gatech.edu

Abstract

This paper reports the fabrication and testing of gold passivated mechanically flexible interconnects (MFIs) with elastic deformation of 65 µm. It is shown that the gold passivation plays a critical role in preserving the lifetime of the flexible interconnects. The gold-passivated MFIs exhibit an unchanged force-displacement characteristic after being vertically indented 100 cycles.

I. Introduction

With continued improvements in IC performance, fine pitch flip-chip bonding, including microbumps, have become ever more critical due to high I/O density, low parasitics, and area-array distribution [1, 2]. Microbumps, in particular, are enabled with the emergence of silicon interposer, which provides a heterogeneous system integration platform. One of the constraints with silicon interposer is that they require a secondary package substrate before being assembled on the motherboard [3]. While there are benefits to be gained if the silicon interposer can be directly mounted on the motherboard, the coefficient of thermal expansion (CTE) mismatch between the large silicon interposer and the organic motherboard (including surface nonplanarity) presents significant challenges (Figure 1). Depending on the application, there may be other challenges, including, for example, interconnect redistribution.

In order to mitigate thermomechanical stresses caused by CTE mismatch and to ensure reliable interconnection, several mechanically flexible interconnects have been proposed for various applications (mostly for die-to-organic package interconnection) that include: 1) modified wire-bond based technology, such as MicroSpring Technology [4]; 2) flexible interconnects formed on or within a low-modulus polymer layer, such as WAVE Package [5], Floating Pads Technology [6], Sea of Leads (SoL) [7]; 3) stress engineered metal interconnects, such as rematable spring interconnect [8], J-spring [9] and coiled micro-spring [10]; and 4) 3D free standing micro-spring technology, such as β-Helix [11], G-Helix [12], Flex Connects [13], NiW micro-springs [14] and curved copper compliant die-package interconnects [15]. With the right mechanically flexible interconnect technology, it may be possible to directly mount a silicon interposer (carrier) on the motherboard, as shown in Figure 1. In [16], a mechanically rigid 'thick' silicon interposer with electrical and optical TSVs was developed. We envision possibly using such mechanically rigid interposers for assembly on the motherboard with the aid of microfabricated flexible interconnects.

Yang *et al*. has previously reported novel 3D-curved flexible interconnects called Mechanically Flexible Interconnects (MFIs) using copper (Cu-MFIs) [17, 18]. However, due to the low yield strength of copper, it is difficult to attain a high range of elastic deformation. This challenge was addressed recently by the use of NiW [19], which exhibits a very high value of yield strength. In [14, 19], the authors reported flexible interconnects based on this material that exhibit large elastic deformation. While this material addresses the yield strength issue, both Cu and NiW readily oxidize making them difficult to use reliably in some applications. In this paper, we extend the work of Yang *et al.* by using the NiW material and passivate the interconnects with electroless gold plating to attain 65 µm elastic deformation and preserve the mechanical deformation characteristics over a test period of two months. With the 65 µm vertical range-of-motion, motherboard non-planarity, CTE mismatch, and other mechanical issues may possibly be compensated for. Of course, the gold passivated MFIs can be used for both temporary interconnect applications, such as in probe cards for wafer-level testing, and for permanent interconnect applications [17, 18].

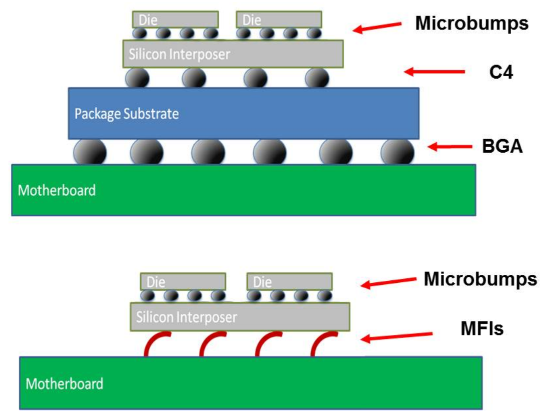

Figure 1: Use of MFIs to enable assembly of a large silicon interposer on an organic substrate

II. Design Aspect of MFIs

Durable MFIs with elastic deformation and high contact force are desirable for a wide range of applications that require temporary interconnection. For example, MFIs can be used in probe cards for wafer-level testing as well as in rematable electronic applications [8]. In order to operate within the elastic deformation range and therefore enable reusability of MFIs, the maximum local internal stress of MFIs during deformation should not exceed the material yield strength, which is defined as the stress beyond which the material starts to deform plastically and cannot recover the original profile. However, given that a relatively large contact force is necessary for temporary interconnection to ensure reliable electrical interconnection, the maximum local internal stress is expected to be relatively large, which might cause plastic deformation. Therefore, a trade-off must be made between the elastic deformation range and the contact force. The following is a brief design strategy adopted for the MFIs under consideration:

-First, form the MFIs by choosing a material with high yield strength, which affords the MFIs to have a large internal stress for a desired contact force while maintaining elastic deformation. This issue is reported in [14, 19].

-Second, follow the design strategy developed in previous work of Yang *et al.* [17, 18] to optimize the 3D tapered and curved geometry of the MFIs to attain a maximum internal stress below the yield strength of the material.

-Third, MFIs must be passivated in order to ensure the reliability in many practical applications. Electroless gold plating is adopted in this work to form the passivation layer.

These points are discussed further below.

A. High Yield Strength Metal Alloy-NiW

Due to the high conductivity and established electroplating techniques, Cu has been used extensively for mechanically flexible interconnects [5-7, 10-13, 17, 18]. However, the yield strength of Cu is less than 121 MPa [20] and thus limits the elastic deformation. Tungsten, although has a high yield strength of ~1.5 GPa [21], cannot be deposited by electroplating and thus limiting its usage. Due to the nano-crystal structure, the NiW alloy developed in [14, 19] is ideal for MFIs as it has a yield strength of up to 1.9 GPa and can be deposited using electroplating. The latter is particularly important since a thick metal layer is typically needed and the electroplating process is compatible with the MFI technology under consideration.

B. Tapered MFI Design

For a given deformation, the internal stress can be lowered by either extending the MFI length or reducing the MFI thickness. Extending the MFI length lowers I/O density and increases electrical parasitics, and thus, is not an ideal solution. Reducing the thickness of MFI significantly lowers the contact force and therefore degrades the reliability of the flexible interconnects. In addition, thinning the MFI increases the resistance, which might not be a serious issue for highly conductive metals, such as Cu, but presents a challenge for lower conductive metals, such as NiW (resistance measurements reported later in the paper).

Based on the principles developed by Yang *et al.* [17, 18], tapered MFI width is used here to distribute the stress more uniformly and provide larger range of motion. Figure 2 illustrates FEM simulation of the stress distribution within a tapered NiW MFI with 50 μm vertical deformation. The simulated MFI is 9 μm thick and occupies a footprint of 120 μm by 200 μm. The FEM simulation was performed using ANSYS Workbench software package. With this much deformation, the maximum local stress is 2.2 GPa, which is close to the yield strength of NiW. The simulated reaction force is 6.0 mN.

Since the gold passivation layer is very thin (≤0.5μm) and soft compared to NiW, the impact of the gold passivation layer on the mechanical deformation of the MFI is neglected in the simulations; experimental data reported later in the paper verify this assumption.

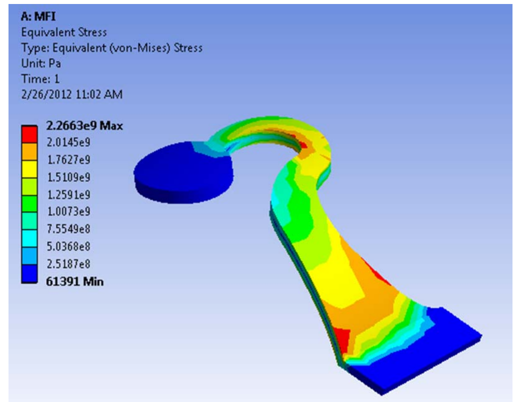

Figure 2: Stress distribution in NiW MFI after being deformed by 50 μm

III. Fabrication Process

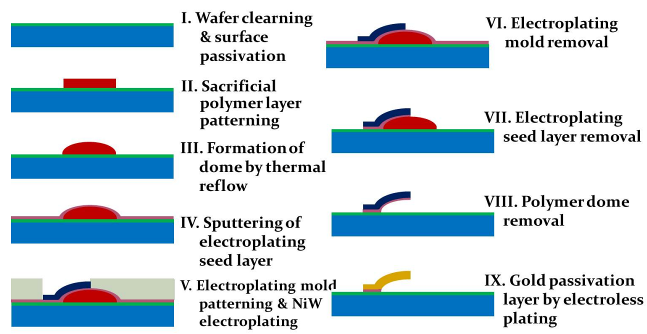

Figure 3: MFI fabrication process

As shown in Figure 3, similar to the Cu-MFI process established in [17, 18], the fabrication of the flexible interconnects under consideration requires only two photolithography steps. The first masking step is used to pattern a sacrificial polymer layer on the substrate, followed by a thermal reflow process to form a dome. The second photolithography step is used to pattern a photoresist electroplating mold on the surface of a Ti/Cu/Ti seed layer that covers the sacrificial polymer. After the electroplating of the NiW MFIs, the electroplating mold, seed layer and sacrificial polymer dome are removed subsequently leaving behind free-standing MFIs with a 120 μm by 200 μm footprint and 65 μm Z-axis gap, as shown in Figure 4 and Figure 5. Finally, a gold passivation layer is deposited on the free-standing MFIs using an electroless plating process.

The gold passivation process step is critical since the durability of the flexible interconnects is strongly dependent on it. Whether Cu or NiW is used to form the MFIs, oxidation and corrosion of the exposed metals to the ambient will result in MFIs with a short lifetime. Therefore, a passivation layer is mandatory for MFIs exposed to the ambient in order to preserve the mechanical and electrical properties during their lifetime.

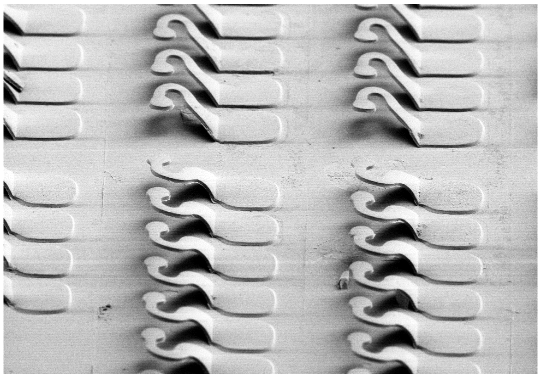

Figure 4: Free standing (65 µm) Au-NiW MFIs

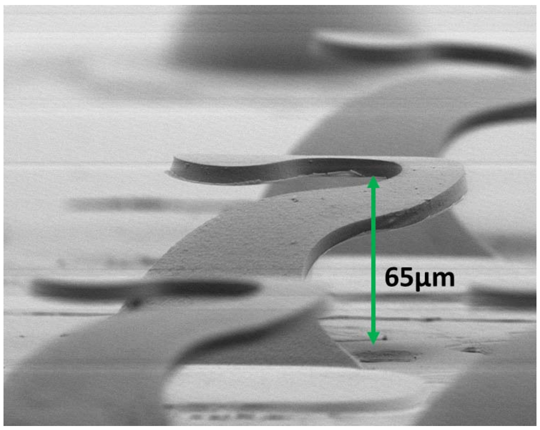

Figure 5: Gold passivated NiW MFIs with 65µm Z-axis gap

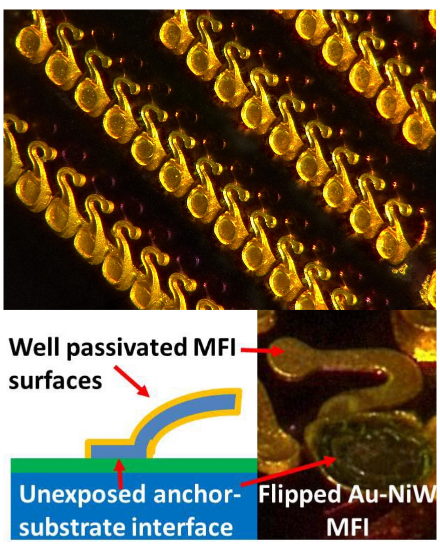

Figure 6: Optical micrograph images of MFIs with 65 µm Z-axis gap after electroless gold passivation layer

Gold electroless plating is adopted in this work to form a passivation layer on the surface of the NiW MFIs, as shown in Figure 6. Compared with other methods for passivation (for example, polymer coating) there are significant benefits: 1) high conductance, which is helpful to lower the MFI resistance especially for NiW MFI, 2) simple and low cost processing since electroless plating requires no photolithography, and 3) longer lifetime, which is experimentally verified later in the paper. During electroless plating, the chemical reaction occurs on all conductive surfaces, as shown in Figure 6, and therefore, all exposed MFI surfaces are passivated (i.e., MFI top and bottom surfaces as well as sidewalls). In order to verify this, one of the gold passivated NiW MFIs was flipped using tweezers (large force was applied to detach the MFI) to illustrate the passivation layer uniformity (Figure 6). The only uncoated part of the MFI, as expected, is the unexposed interface between the anchor of MFI and the substrate.

IV. Results and Discussion

A. Mechanical Characterization

Mechanical properties of Au-NiW MFIs, particularly the maximum elastic deformation range and the corresponding contact force and compliance, are determined by indentation. This section reports the results of the mechanical characterization of the MFIs.

1)Indentation Test of Au-NiW MFIs

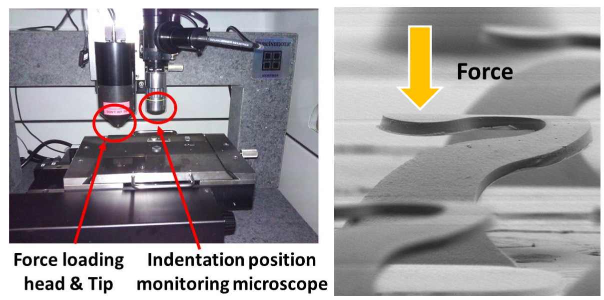

Figure 7: Indentation test tool and setup

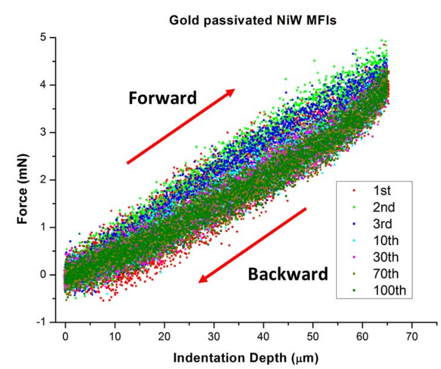

Figure 8: Gold passivated NiW MFI with up to 65 µm elastic deformation (100 indent cycles shown)

Indentation testing of the MFIs is performed using a Hysitron TriboIndenter, as shown in Figure 7. During one indentation cycle, the piezo-driven tip follows a predefined force profile on the free-standing MFI resulting in a downward motion to a preset depth followed by a force release. The real-time position and corresponding reaction force of the tip, which has the same value as that of the MFI, are recorded.

Figure 8 illustrates the results of 100 indentation test cycles performed on a single Au-NiW MFI. Two loading processes are done in each cycle: forward loading and backward loading, which are recorded, respectively, as forward plot and backward plot. During the forward process, the MFI is forced downward by the indentation tool. Similarly, during the backward process, the recovery force and position of the deformed MFI are recorded. Therefore, the elastic deformation of the Au-NiW MFI can be verified by the fact that the forward and backward plots of each cycle overlap and the linear relationship between contact force and indentation depth. The results in Figure 8 demonstrate that the full 65 µm Z-axis gap can be elastically deformed. The contact force is 4 mN since a thin NiW layer was used for the tested MFI. As was indicated in the previous section, in order to increase the contact force, a thicker NiW layer should be deposited. This can of course be easily done since the NiW is electrodeposited.

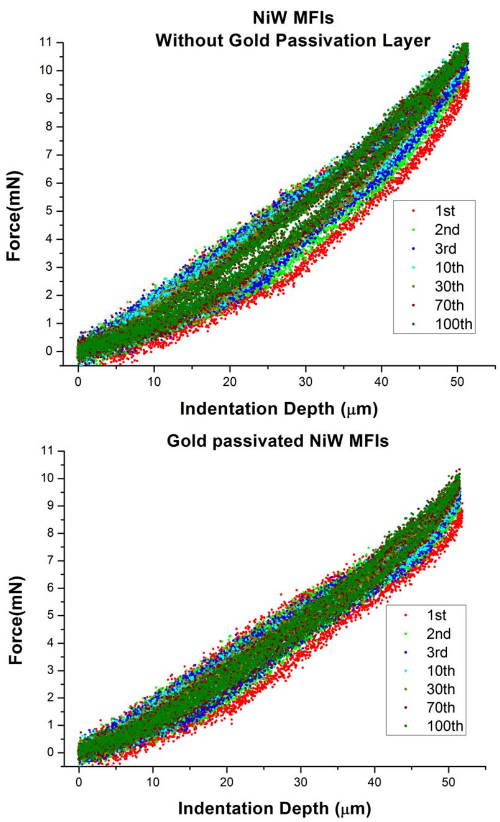

Figure 9: Comparison between (top) NiW MFI and (bottom) Au-NiW MFI

In order to verify that the electroless gold film does not degrade the vertical range of motion of the MFIs, MFIs before and after gold passivation were indented. Figure 9 illustrates the results of a 100 indentation test cycles on NiW MFI before and after gold passivation. The measured anchor thickness of the NiW MFI is 10.12µm, and the corresponding contact force for 50 µm deformation is 10.8 mN (i.e., compliance of 4.63 mm/N). The gold passivated MFI was first cleaned with diluted HCl prior to electroless gold deposition to remove the native oxide from the NiW layer. The anchor thickness of the resulting MFI is 9.43 µm (prior to gold electroless plating) and 9.73 µm after electroless gold plating (i.e., 0.3 µm of electroless gold was deposited). Since both sides of the free-standing MFI are coated with gold, the total thickness of MFI is approximately 10.03µm (i.e., 0.3 µm of gold on both the top and bottom sides of the MFI). Based on the measured indentation results in Figure 9, the corresponding contact force for 50 µm deformation is 10 mN (i.e., compliance of 5mm/N).

Based on the comparison of the two indentation results shown in Figure 9, the impact of the electroless gold passivation layer/process appears to be negligible. From Figure 9, however, it can be seen that the first few indentation cycles are not as linear as the last ones. This is believed to be caused by some plastic deformation that occurs in the first several indentations. These might be caused by minor defects generated during the fabrication process. Once these defects are recovered after the first several indentations, subsequent indentation profiles are almost identical (roughly, from the 10^{th} cycle to the 100^{th} one).

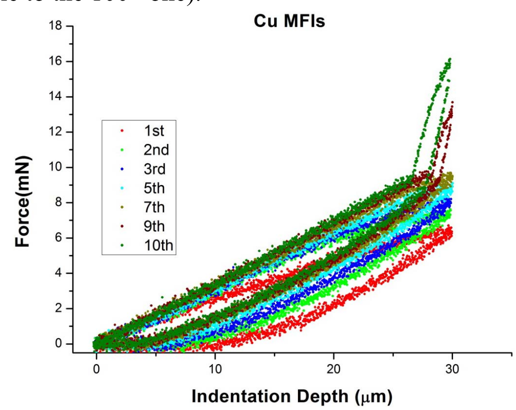

Figure 10: Cu MFI indentation

Cu-MFIs of the same design were also fabricated in order to compare the Au-NiW MFIs to Cu-based MFIs. In this case, the copper was 11 µm thick. As shown in Figure 10, the elastic range of the Cu MFI is less than 30 µm. The forward and backward plots are not overlapped with each other and the contact force is not linear with indentation depth. The Z-axis gap between the MFI top plate and substrate continues to shrink after each indentation cycle due to plastic deformation. The shrinkage can be verified by the backward plot intercept on indentation depth axis, which indicates that the height difference between the starting and end positions of each indentation cycle. With the Z-axis gap decrease caused by plastic deformation, the Z-axis gap of MFI is finally smaller than 30 µm, and the tip of the MFI touches the substrate surface at the end of forward process of the 9^{th} indent. This conclusion is based on the fact that the contact force increases at a much larger slope than prior experiments. Such conclusions agree with the work presented in [14, 19], where the motivation for NiW was developed.

2)Improved lifetime of NiW MFIs

As mentioned earlier, one of the challenges in the development of flexible interconnect technology is that the performance degrades significantly with respect to time if no passivation layer is used to protect the material from

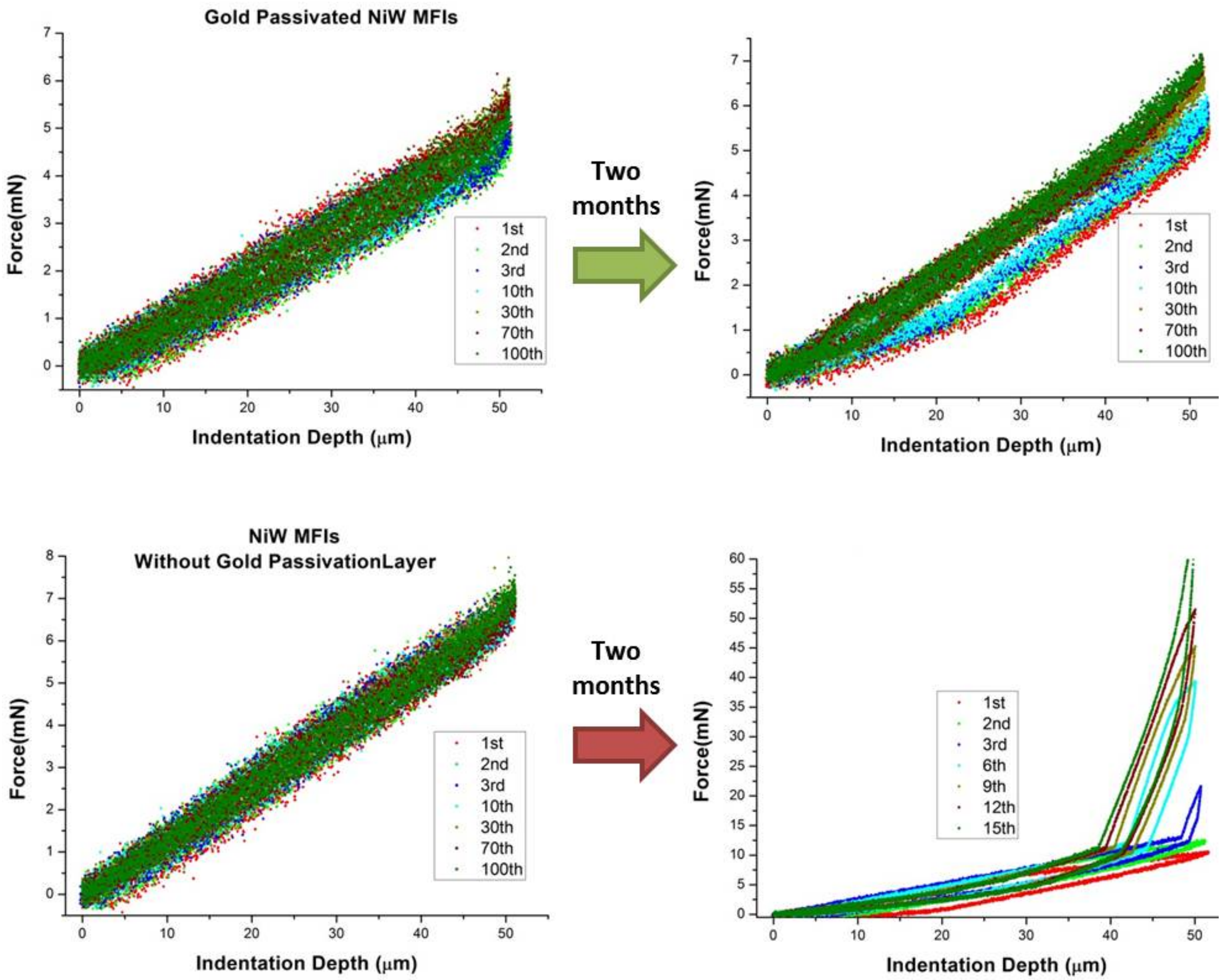

Figure 11: Life-time verification of NiW MFIs with gold passivation layer. NiW MFIs with gold passivation layer maintain the 50 μm elastic deformation capability after two months, unlike the non-passivated NiW MFIs

oxidation. In order to verify the lifetime improvement due to the electroless gold passivation layer, 100 indentation test cycles were carried out on NiW MFIs with and without gold passivation. After testing, the two samples were stored in room temperature with relative humidity of 42% for two months and then indented again. As shown in Figure 11, after two months, the NiW MFIs with electroless gold passivation maintained their >50 μm elastic deformation. However for the NiW MFIs without gold passivation layer, plastic deformation was observed as indicated by the non-overlapped forward and backward plots. In addition, the backward plot intercept on the indentation depth axis shows that the tip of Cu MFI does not return to the starting position of each cycle, which indicates that plastic deformation takes place. The Z-axis gap was shrunk to less than 50 μm (from 65 μm initial gap) after the first two cycles.

B. Electrical Characterization

MFI electrical resistance measurements were carried out using four point probing method, as shown in Figure 12. During the measurements, the tested MFIs are partially deformed to attain a stable resistance reading. Since Cu has lower resistivity than NiW, the resistance of the measured NiW MFIs by four point probing is much higher than the Cu MFI (both MFIs had same design and thickness). The resistance of the NiW MFI, which was 10.25 μm thick, is 101.62 mΩ. This value is higher than the FEM simulated electrical resistance in ANSYS, which was 78.1 mΩ. This difference is believed to be caused by the contact resistance since the partially deformed MFI cannot provide large enough contact force to sufficiently break the thin native oxidation layer on the MFI surface. The measured resistance of the MFIs after electroless gold plating (0.3μm thickness on each side of MFI) is 67.8 mΩ. The resistance drop due to the gold passivation results from two factors: 1) the gold passivation layer provides a low resistance layer in parallel to the NiW film, and 2) the gold passivation layer maintains high conductivity and non-oxidized contact surface to ensure a good contact interface between the probe tip and the MFI. Of course, the electrical resistance of the MFI can be adjusted by forming thicker MFI. Given a target deformation depth, thicker MFI provides larger contact force and lower resistance, which is desirable. However, additional design effort is needed to ensure that the maximum internal stress is lower than the yield strength of the material.

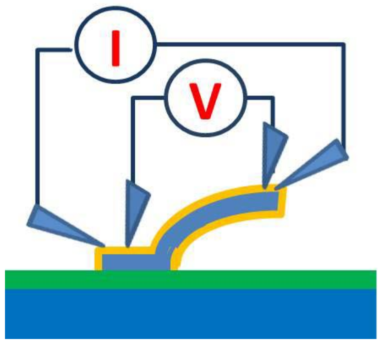

Figure 12: Four-point resistance measurement of MFIs

TABLE I
COMPARISON OF DIFFERENT METAL MFIS

	Cu MFIs	NiW MFIs	Au-NiW MFIs
Resistance (mΩ)	Low	Moderate	Low/ Moderate
Elastic Deformation Range	Low	High	High
Compliance	NA	Stiffer	Stiffer
Lifetime	Short	Short	Excellent

V. Conclusion

Wafer-level batch fabricated gold passivated NiW MFIs with 65 µm vertical elastic range-of-movement are experimentally demonstrated for the first time. Through the use of the gold passivation layer, the large elastic deformation range was preserved for the 2 months lifetime test period. The above set of results are enabled using three key features introduced in this paper: 1) fabrication of MFIs with 65µm Z-axis gap, 2) electrodepostion of high yield-strength NiW on the curved and tapered MFI profile design, and 3) electroless gold passivation layer on the MFIs.

Acknowledgments

We gratefully acknowledge funding from DoD and Oracle Labs.

References

[1] J. Kloeser *et al.*, "Fine pitch stencil printing of Sn/Pb and lead free solders for flip chip technology," *IEEE Trans. Components, Packaging, and Manufacturing Technology, Part C,* 1998, pp. 41-50.
[2] M. Gerber *et al.*, "Next Generation Fine Pitch Cu Pillar Technology – Enabling Next Generation Silicon Nodes," in *Proc. Electronic Components and Technology Conference,* 2011, pp. 612-618.
[3] B. Banijamali *et al.*, "Advanced Reliability Study of TSV Interposers and Interconnects for the 28nm Technology FPGA," in *Proc. Electronic Components and Technology Conference,* 2011, pp. 285-290.
[4] N. Tracy *et al.*, "Array Sockets and Connectors Using MicroSpring™ Technology," *Twenty-Sixth IEEE/CPMT International Electronics Manufacturing Technology Symposium*, 2000, pp. 129-140.
[5] Y.-Kim *et al.*, "Wide area vertical expansion (WAVE) package design for high speed application: reliability and performance," in *Proc. Electronic Components and Technology Conf.*, 2001, pp. 54–62.
[6] R. Fillion *et al.*, "On-wafer process for stress-free area array floating pads," in *Proc. Int. Symp. Microelectronics*, 2001, pp. 100–105.
[7] M. Bakir *et al.*, "SoL Ultra high density wafer level chip input/output interconnections for gigascale integration (GSI)," *IEEE Trans Electron Devices,* 2003, pp. 2039-2048.
[8] I. Shubin *et al.*, "Novel packaging with rematable spring interconnect chips for MCM," in *Proc. Electronic Components and Technology Conf,* 2009, pp. 1053-1058.
[9] L. Ma *et al.*, "J-springs innovative compliant interconnects for next-generation packaging," in *Proc. Electronic Components and Technology Conference,* 2002, pp. 1359-1365.
[10] R. Marcus *et al.*, "A new coiled microspring contact technology," in *Proc. Electronic Components and Technology Conference*, 2001, pp. 1227-1232.
[11] Q. Zhu *et al.*, "β-Helix: A Lithography-Based Compliant Off-Chip Interconnect," *IEEE Trans. Components and Packaging Technology,* 2003, pp. 582-590.
[12] Q. Zhu *et al.*, "Design and optimization of a novel compliant off-chip interconnect one-turn helix," in *Proc. Electronic Components and Technology Conference*, 2002, pp. 910-914.
[13] K. Kacker *et al.*, "FlexConnects: A Cost-Effective Implementation of Compliant Chip-to-Substrate Interconnects," in *Proc. Electronic Components and Technology Conference*, 2007, pp. 1678-1684.
[14] G. Spanier *et al.*, "Platform for Temporary Testing of Hybrid Microsystems at High Frequencies," *J. MEMS* 2007, pp. 1367-1377.
[15] S. Muthukumar *et al.*, "High-Density Compliant Die-Package Interconnects," in *Proc. Electronic Components and Technology Conference*, 2006, pp. 1233-1238.
[16] M. Parekh *et al.*, "Electrical, Optical and Fluidic Through-Silicon Vias for Silicon Interposer Applications," in *Proc. Electronic Components and Technology Conference*, 2011, pp. 1992-1998.
[17] H. Yang *et al.*, "3D integration of CMOS and MEMS using mechanically flexible interconnects (MFI) and through silicon vias (TSV)," in *Proc. Electronic Components and Technology Conference*, 2010, pp. 822-828.
[18] H. Yang *et al.*, "Design, Fabrication, and Characterization of Freestanding Mechanically Flexible Interconnects Using Curved Sacrificial Layer," *IEEE Trans. on Components, Packaging and Manufacturing Technology,* 2012 (electronic version published on Jan 4^{th}, 2012 on IEEE Xplore).
[19] E. Slavcheva *et al.*, "Electrodeposition and properties of NiW films for MEMS application," *Electrochimica Acta* Vol.50, 2005, pp. 5573–5580.
[20] R. Iannuzzelli "Predicting plated-through-hole reliability in high temperature manufacturing processes," in *Proc. Electronic Components and Technology Conference,* 1991, pp. 410-421.
[21] http://en.wikipedia.org/wiki/Ultimate_tensile_strength